Diffusion Tensor Imaging of the Normal Pediatric Spinal Cord Using an Inner Field of View Echo-Planar Imaging Sequence

N. Barakat, F.B. Mohamed, L.N. Hunter, P. Shah, S.H. Faro, A.F. Samdani, J. Finsterbusch, R. Betz, J. Gaughan and M.J. Mulcahey

AJNR Am J Neuroradiol 2012, 33 (6) 1127-1133
doi: https://doi.org/10.3174/ajnr.A2924
http://www.ajnr.org/content/33/6/1127

ORIGINAL RESEARCH

Diffusion Tensor Imaging of the Normal Pediatric Spinal Cord Using an Inner Field of View Echo-Planar Imaging Sequence

N. Barakat
F.B. Mohamed
L.N. Hunter
P. Shah
S.H. Faro
A.F. Samdani
J. Finsterbusch
R. Betz
J. Gaughan
M.J. Mulcahey

BACKGROUND AND PURPOSE: DTI in the brain has been well established, but its application in the spinal cord, especially in pediatrics, poses several challenges. The small cord size has inherent low SNR of the diffusion signal intensity, respiratory and cardiac movements induce artifacts, and EPI sequences used for obtaining diffusion indices cause eddy-current distortions. The purpose of this study was to 1) evaluate the accuracy of cervical spinal cord DTI in children using a newly developed iFOV sequence with spatially selective 2D-RF excitations, and 2) examine reproducibility of the DTI measures.

MATERIALS AND METHODS: Twenty-five typically developing subjects were imaged twice using a 3T scanner. Axial DTI images of the cervical spinal cord were acquired with this sequence. After motion correction, DTI indices were calculated using regions of interest manually drawn at every axial section location along the cervical spinal cord for both acquisitions. Various DTI indices were calculated: FA, AD, RD, MD, RA, and VR. Geometric diffusion measures were also calculated: Cp, Cl, and Cs.

RESULTS: The following average values for each index were obtained: FA = 0.50 ± 0.11; AD = 0.97 ± 0.20 × 10^{-3}mm^2/s; RD = 0.41 ± 0.13 × 10^{-3}mm^2/s; MD = 0.59 ± 0.15 × 10^{-3}mm^2/s; RA = 0.35 ± 0.08; VR = 0.03 ± 0.00; Cp = 0.13 ± 0.07; Cl = 0.29 ± 0.09; and Cs = 0.58 ± 0.11. The reproducibility tests showed moderate to strong ICC in all subjects for all DTI parameters (ICC>0.72).

CONCLUSIONS: This study showed that accurate and reproducible DTI parameters can be estimated in the pediatric cervical spinal cord using an iFOV EPI sequence.

ABBREVIATIONS: 2D-RF = 2-dimensional radio frequency; AD = axial diffusivity; Ci = confidence interval; Cl = linear index; Cp = planar index; Cs = spherical index; FA = fractional anisotropy; ICC = intraclass correlation coefficient; iFOV = inner field of view; ISNCSCI = International Standards for Neurological Classification of Spinal Cord Injury; MD = mean diffusivity; RA = relative anisotropy; RD = radial diffusivity; SCI = spinal cord injury; VR = volume ratio

Each year, an estimated 11,000 new spinal cord injuries occur in the United States. Among these injuries, 1%–5.4% are reported in children.[1] Although spinal trauma is relatively infrequent in pediatric patients compared with adults, disability and mortality rates are higher: 40% in pediatric patients versus 20% in adults.[2,3] Due to the distinctive biomechanics and anthropometrics of children's spinal cords, 60%–80% of all pediatric cord injuries are cervical.[4] Despite the continued improvements in treatment that help many children survive SCI, most injuries will cause permanent disability. Therefore, continued research is needed to assess neurologic damage after traumatic SCI and to improve care, treatment, and rehabilitation methods.

Currently, the evaluation and classification of neurologic impairment in adults and children with SCI is assessed using the ISNSCI published by the American Spinal Injury Association.[5] These standards involve the testing of sensory and motor function of the limbs, trunk, and anorectal area, and are used to predict recovery of neurologic function, plan treatment, and determine treatment effectiveness. Although internationally recognized, the ISNSCI standards have low utility in the pediatric population and can lead to unreliable assessment of neurologic abnormalities. A recent study has shown that children younger than 6 years of age were unable to understand and follow test instructions, children as old as 10 years were extremely anxious during the examination, and adolescents as old as 15 years withdrew from the study due to discomfort with the anal examination.[6] In addition, these examinations do not provide a direct assessment of damage to white matter tracts within the spinal cord. This can present a considerable challenge against the development of effective treatment approaches designed specifically at the cord level. Therefore, an objective assessment of the spinal cord may provide important information complementary to conventional clinical assessment and may lead to accurate prognostic evaluation of recovery from SCI.

DTI is a promising technique of examining the spinal cord in vivo. It quantifies the diffusion of water molecules in each voxel of an image in directions parallel and transverse to the plane of neuronal axons. The quantitative characteristic of DTI allows the characterization of physical properties of tissues. The unique characteristic architecture of the spinal cord

Received July 11, 2011; accepted after revision September 5.

From the Departments of Bioengineering (N.B.) and Radiology (N.B., F.B.M., L.N.H., P.S., S.H.F.), Temple University, Philadelphia, Pennsylvania; Shriners Hospital for Children (A.F.S., R.B., M.J.M.), Philadelphia, Pennsylvania; Department of Systems Neuroscience (J.F.), University Medical Center Hamburg-Eppendorf, Hamburg, Germany; and Biostatistics Consulting Center (J.G.), Temple University School of Medicine, Philadelphia, Pennsylvania.

This study was funded by the Shriners Hospitals for Children Grant 8956 (Mulcahey, PI).

Paper previously presented in part at: the International Society of Magnetic Resonance in Medicine, Montreal, Quebec, Canada, May 11, 2011.

Please address correspondence to Feroze B. Mohamed, Department of Radiology, Temple University School of Medicine, 3401 N. Broad St, Philadelphia, PA 19140; e-mail: feroze@temple.edu

http://dx.doi.org/10.3174/ajnr.A2924

may allow DTI to localize white matter, separate white from gray matter, and assess structural damage of the cord. Previous studies reported the success of DTI in characterizing different tissues of the spinal cord and demonstrated changes in diffusion characteristics along injured spinal cords.[7-9]

DTI of the spinal cord is technically limited by various factors. The small cord volume (approximately 1 cm in diameter) leads to a low SNR. CSF pulsation and blood flow can produce prominent ghosting artifacts and degrade image quality. The spinal cord is also subject to respiratory and cardiac movements, which cause image blurring and increased or decreased signal intensity. Different tissue interfaces (bone, soft tissue, or fluid) can create susceptibility artifacts. Swallowing or related motion artifacts are mostly seen when imaging the cervical spinal cord.[10,11] Finally, in pediatric imaging especially, the possibility of increased subject motion makes obtaining accurate and reproducible DTI parameter values difficult.[12,13] Artifact-reducing techniques can be used to overcome some of these issues. However, particularly in pediatric imaging, these techniques are not without challenges. Cardiac gating and respiratory compensation may increase acquisition time, and sedation is typically not desirable in children. Thus, fast, reliable, and high-resolution imaging is needed to image pediatric subjects.

Ideally, the goal is to obtain high-resolution artifact-free and reproducible images within minimal scan time. The choice of optimal pulse sequences in pediatric spinal cord DTI is therefore critical. The pulse sequences of choice have been EPI-based designs. While these sequences offer short acquisition times, which reduce motion-related artifacts, they are highly sensitive to susceptibility artifacts and eddy-current distortions.[14,15] Recent work using reduced FOV imaging sequences showed great reduction in geometric distortions when imaging the spinal cord.[16-19] This approach takes advantage of the small-diameter spinal cord morphology and applies a relatively small rectangular FOV to the area of interest. In addition to pulse sequence choice, correcting motion-related artifacts may be a useful step in data analysis and can improve image quality. Artifact-reduction techniques can be applied during data acquisition, which may increase imaging time or the postprocessing stage.

While studies on diffusion imaging of the spinal cord in adults,[7,20,21] as well as in animal models[22-25] have been reported, a comprehensive study of the pediatric spinal cord that examines the accuracy and reproducibility of DTI measures has not yet been reported. The investigation of normative data of spinal cord DTI represents an additional important area of inquiry. The clinical significance of this study is 2-fold. First, as in any imaging study, a thorough understanding of the diffusion characteristics of the healthy spinal cord is essential for the clinical interpretation of images of the injured spinal cord. If DTI proves to be a feasible, accurate, and reliable method for quantifying diffusion changes in the pediatric spinal cord, it may be a useful neurodiagnostic supplement to conventional MR imaging. Second, normative DTI values will provide a basis for which to compare DTI values from children with spinal injuries, allowing for classification of the consequence of injury based on deviation from normal values. Therefore, the purpose of this study is to investigate DTI of the pediatric cervical spinal cord in healthy controls by 1) evaluating the accuracy of DTI in children using a newly developed iFOV sequence with spatially selective 2D-RF excitations, and 2) examining the reproducibility of the DTI measures.

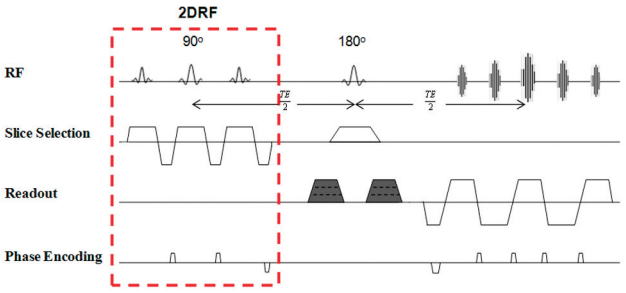

Fig 1. Schematic timing diagram of the diffusion sequence encoding scheme. The iFOV EPI sequence was based on 2D-RF excitations as described in Finsterbusch.[18]

Materials and Methods

Subjects

Twenty-five subjects (6 males and 19 females), with a mean age of 13.28 years (range 7–21 years), were recruited. The age range up to and including 21 years of age represents the ages of youth typically cared for by centers specializing in SCI. The subjects had no evidence of spinal cord injury or pathology. Subjects and their parents provided written informed assent and consent of the institutional review board–approved protocol. Data from 3 subjects were excluded from the analysis—2 due to excessive motion artifacts and 1 with an incidental finding of Chiari I malformation in the cervical spinal cord. Data from the remaining 22 control subjects were included in the analysis.

Imaging

The scans were performed using a 3T Verio MR scanner (Siemens, Erlangen, Germany) with a 4-channel neck matrix and an 8-channel spine matrix coil. All subjects underwent 2 identical scans (mean time = 9 hours). The protocol consisted of conventional sagittal FSE T1- and T2-weighted scans, axial FSE T2-weighted scans, as well as axial DTI acquisition with the iFOV sequence. Anesthesia was not administered to the subjects. Cardiac and respiratory gating were not used.

DTI Acquisition Using iFOV Sequence

The iFOV sequence used in this study was based on a single-shot EPI sequence for diffusion-weighted imaging with spatially 2D-RF excitations. Details regarding this pulse sequence can be found in Finsterbusch's article.[18] In summary, the section-select radio-frequency excitation of a standard EPI sequence was replaced by 2D-RF excitation targeting a rectangular profile, the inner FOV, using a blipped-planar trajectory applied in the phase-encoding direction (Fig 1). The side excitations were positioned outside of the imaged object. To avoid aliasing of the profile's transition region, oversampling of the iFOV in the phase encoding was performed (Fig 2). The iFOV sequence was implemented on the scanner and, during a pilot phase, was optimized for imaging the pediatric spinal cord. Imaging was performed using several diffusion directions (6, 12, 20, and 30), multiple signal intensity averages (1 to 4), different b-values (0, 700, 800, 900, 1000, and 1200 seconds/mm^2), and with cardiac gating. The optimization ensured fast scanning time while maintaining high spatial resolution to delineate the small anatomy. The axial DTI images were acquired in

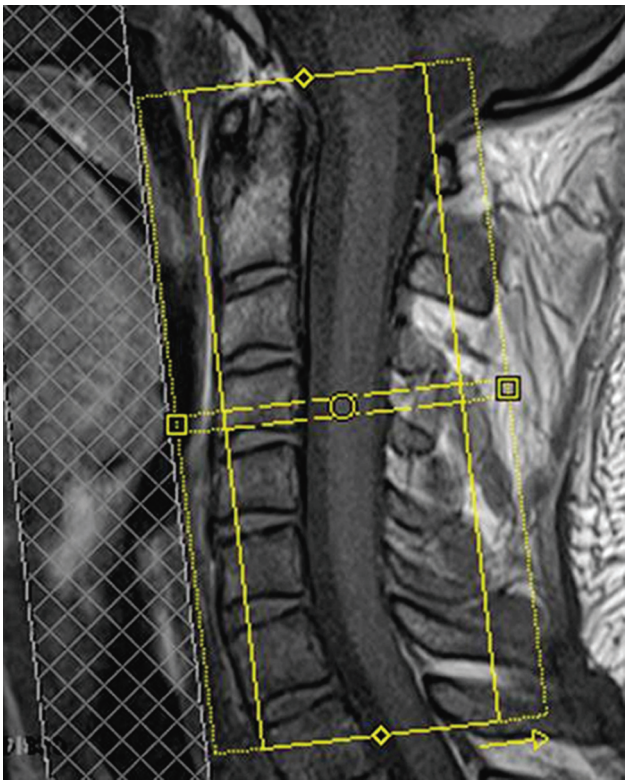

Fig 2. Localization image from which the axial cervical spinal cord image sections were prescribed. The inner solid yellow rectangular line represents the iFOV, which was oversampled (dotted yellow line) to avoid aliasing. A saturation band was applied to reduce flow-related artifacts.

the same anatomic location prescribed for the T2-weighted images to cover the entire cervical spinal cord (C1 to T1 levels). The final imaging parameters included 20 diffusion directions, $b = 1000\text{s/mm}^2$, voxel size = $1.2 \times 1.2 \times 3\ \text{mm}^3$, axial sections = 35–45 (depending on the subject's height), TR = 6100–8000 ms, TE = 115 ms, number of averages = 3, and acquisition time = 7 minutes.

Preprocessing

Initially, the diffusion datasets were corrected for motion-induced artifacts using the AIR image registration package (http://bishopw.loni.ucla.edu/AIR5/index.html) implemented in DTIstudio (http://www.mristudio.org). The target images (20 directional images) were aligned with the reference image (B0) using a rigid registration algorithm and scaled-least-squares cost function.[26]

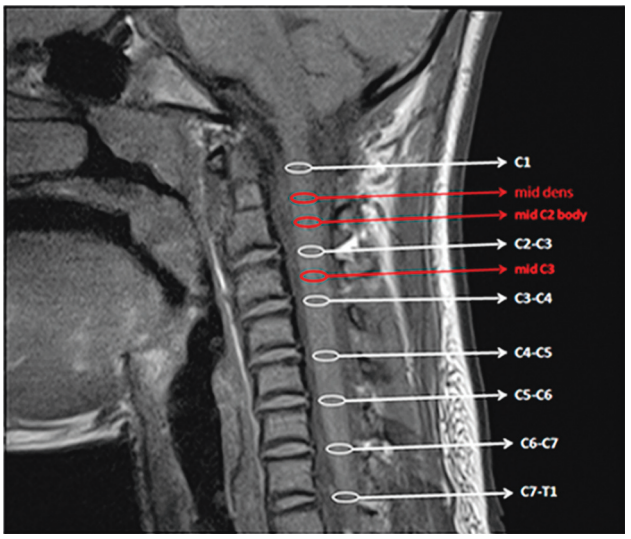

Fig 4. DTI parameters obtained at disk and midlevel locations of the cervical spinal cord.

Tensor Estimation

After motion correction of the diffusion-weighted images, the eigenvectors and eigenvalues of the diffusion tensor matrix were computed on a voxel-by-voxel basis from the axial DT images using MedINRIA software (http://www.sop.inria.fr/asclepios/software/MedINRIA/). Various DTI indices were calculated and tabulated, namely, FA, AD, RD, MD, RA, and VR.[10,27,28]

Tensor Visualization

In addition to the DTI metrics, the following geometric diffusion measures were also extracted: Cp, Cl, and Cs. These visualization indices relate to the geometric shape of the diffusion tensor and may help examine the 3D process of diffusion and fully characterize tissue microstructure.[29-31]

Regions of Interest

For both acquisitions, regions of interest were manually drawn on color FA maps at every axial section location along the cervical spinal cord and were validated by a neuroradiologist to ensure proper anatomic localization. There was a consistent sparing of the outer margin of the cervical cord that represented approximately 1 voxel width to minimize volume averaging with the CSF (Fig 3). Regions of interest were consistently defined throughout all sections. DTI indices were reported at each disk level of the cervical spinal cord as well as the middle (mid) portion of the cervical vertebral body (Fig 4). The values

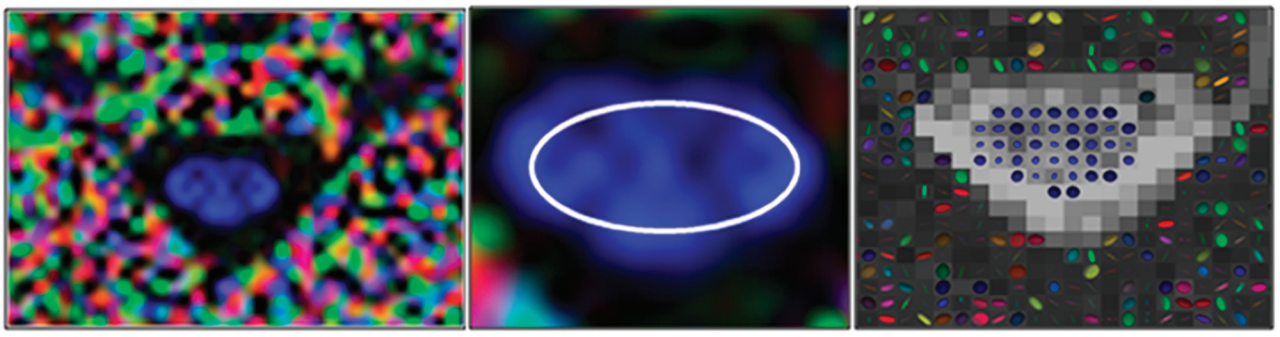

Fig 3. Axial FA color image of a control subject's cervical spinal cord (left). Manual placement of region of interest (middle). Diffusion tensor ellipsoid representation in white and gray matter (right). There was clear discrimination between the butterfly-shaped gray matter and surrounding white matter.

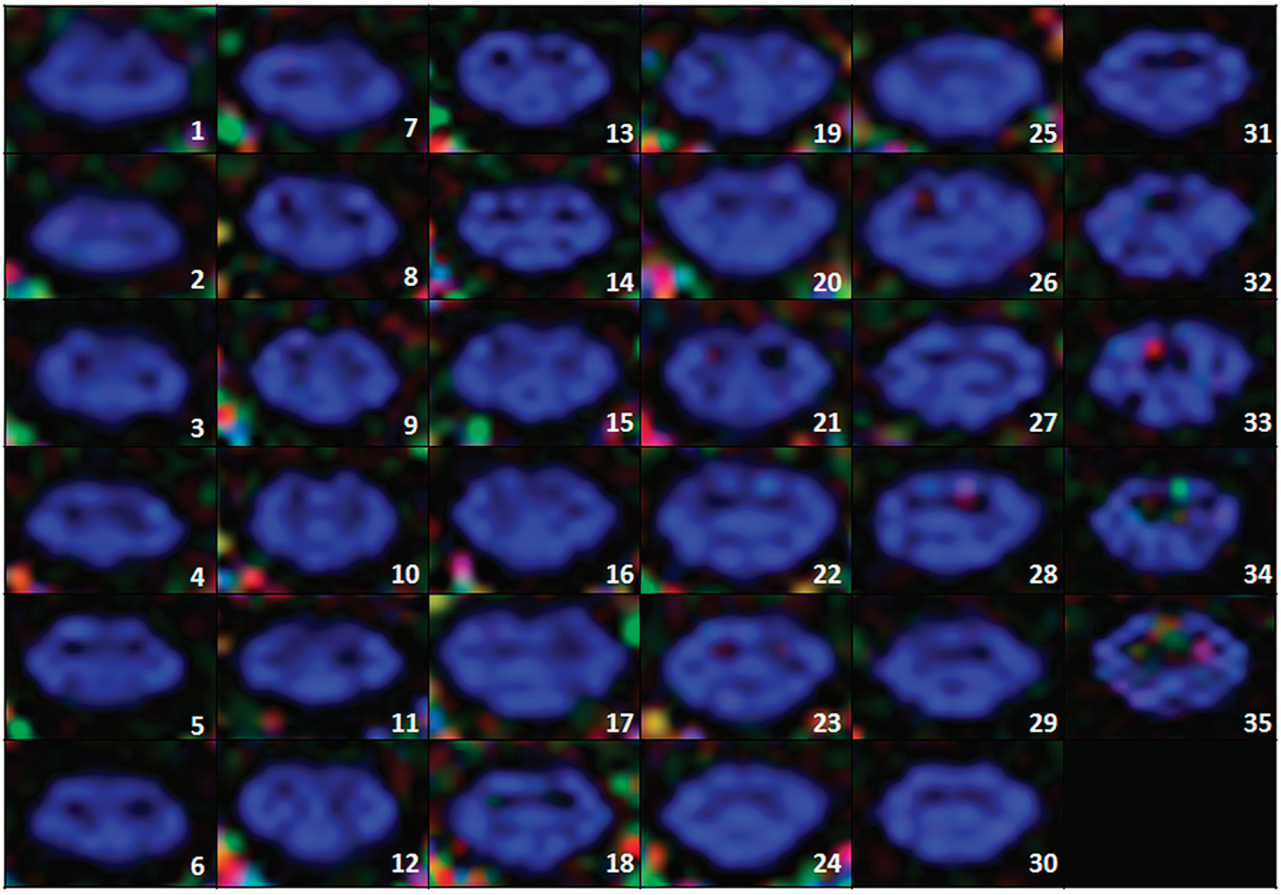

Fig 5. Axial FA color maps along the cervical spinal cord of a control subject (35 sections). Section 1 represents the inferior portion of the cervical cord (C7-T1). Section 35 represents the posterior portion of the cervical cord (C1).

of each DTI parameter were averaged per cord level across all subjects.

Statistics

Statistical analysis was performed to test the reliability of the datasets from the 2 separate scans per subject. This was assessed by calculating the ICC coefficients[32] for each DTI parameter for the entire cervical spinal cord as well as per cord level.

Results

Imaging with the iFOV sequence resulted in high spatial resolution of DT images. Minimal eddy-current distortions and distinctive delineation of gray and white matter structures were observed in most axial sections (Fig 5). Qualitative examination of image registration results showed reduction in motion-induced artifacts and well-defined CSF and cord structures (Fig 6).

The subjects showed mean ± standard deviation FA = 0.50 ± 0.11, AD = 0.97 ± 0.20 × 10^{-3} mm^2/s, RD = 0.41 ± 0.13 × 10^{-3} mm^2/s, MD = 0.59 ± 0.15 × 10^{-3} mm^2/s, RA = 0.35 ± 0.08, VR = 0.03 ± 0.00, Cp = 0.13 ± 0.07, Cl = 0.29 ± 0.09, and Cs = 0.58 ± 0.11. The mean ± standard deviation of each DTI parameter, as a function of cord level, is illustrated in Figs 7 and 8. There was a variation in the parameter values along the spinal cord. Between C1 and T1 levels, there was a progressive decrease in FA (15%), AD (16%), MD (9%), RA (23%), and Cl (27%), and a demonstrated increase in RD (1%), VR (11%), Cp (36%), and Cs (7%).

Reliability tests showed moderate to strong agreement between the 2 scans in all the subjects for all DTI parameters. For the averaged DTI parameter values across all levels, the ICCs and their 95% Cis were FA [ICC = 0.87, Ci (0.78–0.97)], AD [ICC = 0.97, Ci (0.92–0.99)], RD [ICC = 0.91, Ci (0.83–0.98)], MD [ICC = 0.95, Ci (0.92–0.98)], RA [ICC = 0.93, Ci (0.88–0.98)], VR [ICC = 0.82, Ci (0.69–0.95)], Cp [ICC = 0.77, Ci (0.58–0.95)], Cl [ICC = 0.91, Ci (0.85–0.97)] and Cs [ICC = 0.72, Ci (0.50–0.94)]. The ICCs for each DTI parameter as a function of cord level were also assessed and summarized in the Table.

Discussion and Conclusion

DTI can offer a comprehensive understanding regarding structural anisotropy of axonal white matter in any tissue. Diffusion measurement is particularly promising in the spinal cord because the inherent direction of anisotropy is aligned with the cord. In the pediatric spinal cord, the utility of DTI in quantifying diffusion changes has not been well studied. The small volume of the cord, CSF flow, cardiac/respiratory activity, and susceptibility artifacts from adjacent bony structures limit the accuracy and reproducibility of DTI values. Additional challenges include keeping a child motionless for several minutes without the use of sedation and the absence of normative DTI data for comparison. Although diffusion changes in the pediatric brain have been reported,[33-35] no comprehensive study of the pediatric spinal cord has been conducted.

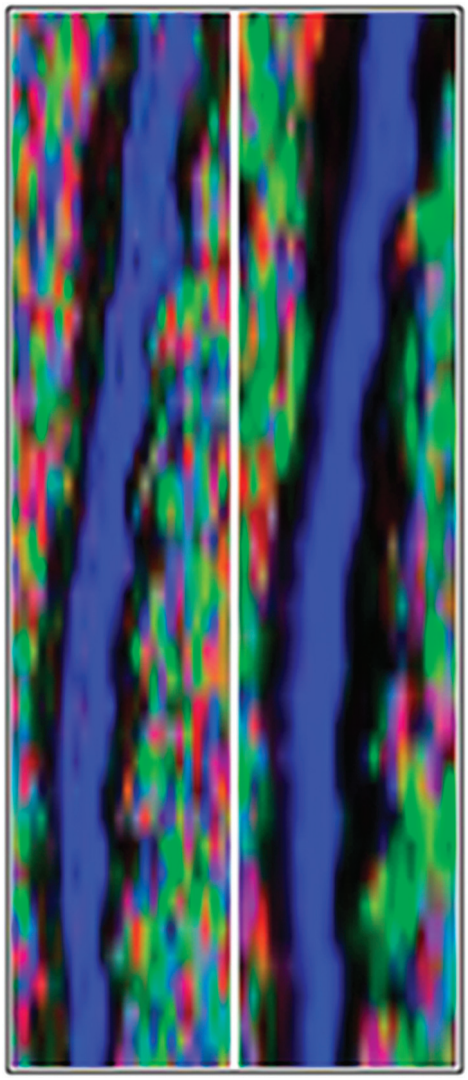

Fig 6. Midline sagittal FA color maps of a representative cervical spinal cord pre- (left) and post- (right) image registration. Noticeable reduction in motion-related artifacts and good CSF versus white matter delineation are observed on the postmotion-corrected image.

Despite these difficulties, DTI parameters were successfully obtained in this study using a well-optimized scanning protocol. The protocol consisted of T1- and T2-weighted sequences, as well as an iFOV single-shot EPI sequence for DTI acquisition. The iFOV was installed on the MR imaging scanner and pilot tested on phantom models and adult subjects, as well as children to optimize scanning parameters. The scans were performed using several diffusion directions, multiple signal intensity averages, different b-values, and with cardiac gating. Qualitative assessments of the images and SNR calculations were performed for each combination of parameters. The optimal pulse sequence parameters were chosen based on maximum spatial resolution and maximum SNR while maintaining good image quality and minimum scan time. For axial acquisition of the pediatric cervical spinal cord (35–45 sections), the scan time was determined to be approximately 8 minutes.[14] When cardiac gating was used, there was no significant improvement in either SNR or image quality. There was, however, a significant increase in scan duration (>60%), which exceeded acceptable scan time limit. Therefore, cardiac gating was not incorporated in this study. The optimization and testing of the iFOV sequence parameters led to an increase in image resolution while maintaining a short scan time. As a result, the gray and white matter structures could be clearly visualized across cord sections for most subjects (Fig 5).

Incorporating motion correction at the postprocessing stage before DTI analysis also proved to be valuable in data analysis. This step was accomplished via image registration using AIR with a rigid body transformation technique. This registration method uses information taken from the reference image (B0 in this case) and the target images (20 gradient directions) and creates a cost function, which quantifies the amount of mutual information between the images. Rigid body registration assumes the movement of the imaged area is rigid (free of deformation). It is commonly used in medical applications where the imaged structure is assumed to be encased within a bony structure (eg, the brain).[36] As a result, the rigid body registration method was chosen in this study because the spinal cord is also encased and protected by a bony structure—the vertebral column. Furthermore, a study investigating quantitative and qualitative analysis of several image registration methods showed that the rigid registration technique was superior to other registration methods.[26] Although the image registration approach was effectively capable of reducing artifacts caused by rigid displacement of the spinal cord, particularly motion in the anteroposterior direction, some motion-related artifacts remained: CSF pulsation, sporadic swallowing, and subject bulk motion.

With the absence of any studies or results of DTI in the pediatric spinal cord, this test–retest methodology was used to ensure accurate and reproducible quantification of diffusion changes in the spinal cord. Reliability of a quantitative imaging test is a critical feature that may allow for monitoring in vivo changes due to disease progression and treatment effectiveness. Poor reproducibility limits the potential clinical application of any medical imaging technique. To evaluate the reproducibility of these results, all subjects were scanned twice, using the same acquisition protocol, within an average time interval of 9 hours. No scanner upgrades were performed during the length of the study. Image registration and DTI analysis methods were identical in both datasets, and the regions of interest were drawn the second time by the same observer. The reproducibility of the different DTI parameters was evaluated using the ICC and showed moderate to strong agreement between the repeated-measurements scans (0.72–0.97). However, examining the ICC values as a function of cord level revealed slight fluctuations in lower levels. Signal intensity drop-offs at the edge of the neck coil may have been a contributing factor to these differences because the lower cervical and upper thoracic levels were positioned at the extremities of the neck coil, where SNR decreases.

The results of this study showed a gradual decrease in FA, AD, MD, RA, and Cl values, and a gradual increase in VR, Cp, and Cs values along the length of the spinal cord in the superior to inferior direction (C1 to T1), while RD remained relatively constant. This variations pattern can be attributed to the following effects:

1) In the upper cervical spinal cord, there is a higher attenuation of large-diameter axons compared with the upper thoracic region and, consequently, an increased axial (or longitu-

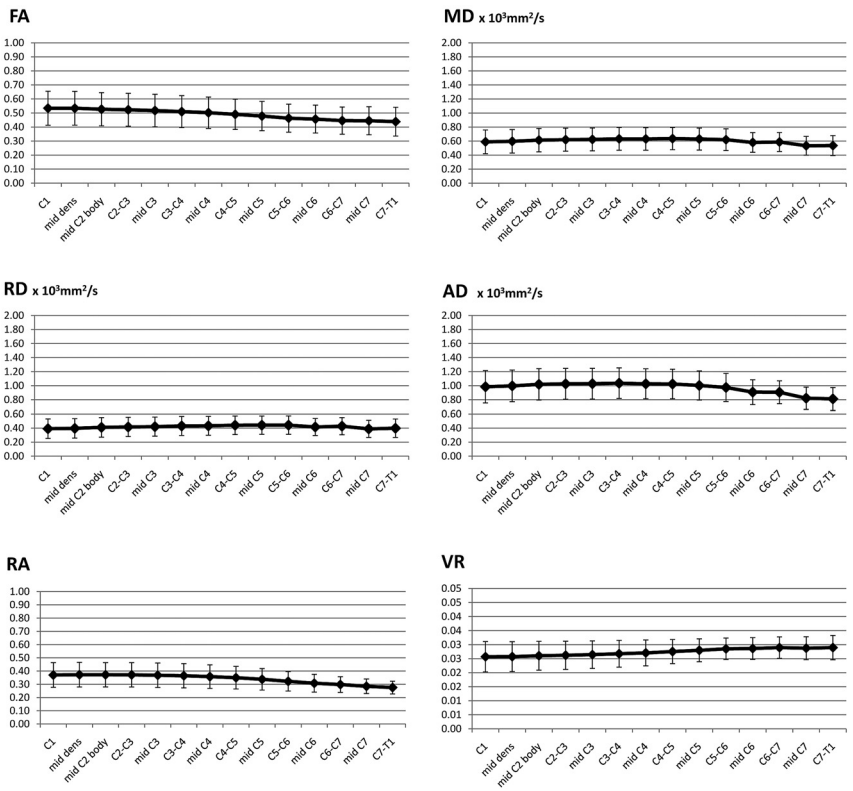

Fig 7. DTI parameters values averaged across all the controls and plotted as a function of cord levels. Data from 1 measurement are shown. The error bars represent the standard deviations.

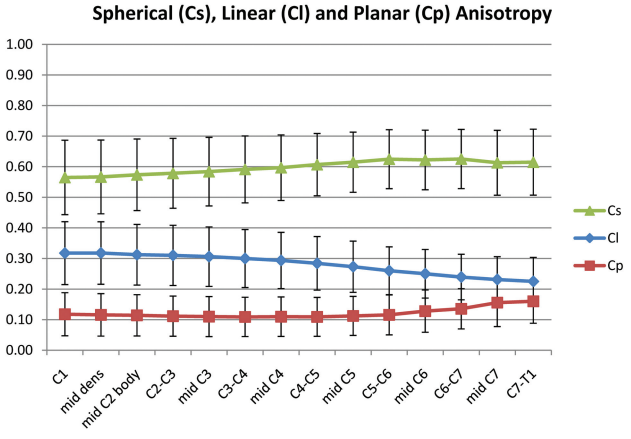

Fig 8. Tensor visualization indices (Cs, Cl, and Cp) averaged across all the controls and plotted as a function of cord levels. Data from 1 measurement are illustrated. The error bars represent the SDs.

ICCs of all DTI indices per cord level

	FA	AD	RD	MD	RA	VR	Cl	Cp	Cs
C1	0.59	0.73	0.70	0.68	0.66	0.62	0.65	0.42	0.41
Mid dens	0.55	0.70	0.69	0.70	0.59	0.51	0.57	0.45	0.34
Mid C2 body	0.55	0.73	0.73	0.71	0.59	0.53	0.61	0.47	0.39
C2-C3	0.56	0.76	0.76	0.76	0.65	0.54	0.65	0.50	0.45
Mid C3	0.61	0.77	0.76	0.76	0.63	0.56	0.65	0.55	0.45
C3-C4	0.58	0.76	0.74	0.76	0.59	0.54	0.65	0.51	0.41
Mid C4	0.59	0.75	0.71	0.73	0.57	0.56	0.66	0.44	0.41
C4-C5	0.63	0.71	0.69	0.72	0.57	0.58	0.66	0.38	0.43
Mid C5	0.57	0.65	0.64	0.68	0.55	0.52	0.62	0.43	0.35
C5-C6	0.58	0.59	0.61	0.61	0.51	0.51	0.63	0.39	0.45
Mid C6	0.62	0.51	0.39	0.39	0.51	0.63	0.67	0.50	0.50
C6-C7	0.68	0.48	0.46	0.51	0.59	0.58	0.72	0.44	0.44
Mid C7	0.70	0.56	0.45	0.54	0.62	0.59	0.78	0.16	0.38
C7-T1	0.43	0.61	0.48	0.57	0.51	0.23	0.61	0.25	0.00

dinal) diffusivity (AD).[34,35] Subsequently, all the DTI indices (FA, MD, RA, and Cl) that are proportionally related to AD also showed a decrease in the thoracic region, and the parameters that are inversely proportional to AD showed an increase. This pattern is similar to that reported in other studies involving adult subjects.[20,37]

2) The geometric shape of the diffusion tensor is assumed to be ellipsoid and the 3 eigenvalues (λ_1, λ_2, and λ_3) corresponding to diffusivities along the principal axes of the diffusion tensor are sorted in the order $\lambda_1 \gg \lambda_2 \sim \lambda_3$. In a highly anisotropic axonal-shaped medium, AD represents diffusivity along the primary axis of the diffusion tensor parallel to the spinal cord tracts (AD = λ_1). RD represents diffusivity perpendicular to the spinal cord tracts and is the average of λ_2 and λ_3. It was therefore expected that RD would remain constant across cord levels.

3) Cardiac gating was not used in this study. The lowest cervical levels (C4–C7) are the most sensitive to cardiac motion.[10,11] Therefore, some cardiac-related artifacts may have biased the quantification of DTI parameters. While this may be considered a limitation in the study, it is important to note that gating increases acquisition time and does not prevent subject motion. Keeping the acquisition time relatively short was a priority for imaging the pediatric population.

Another potential limitation in the study is the sex- and age-dependent variances in the data. Previous studies on DTI in brain white matter reported differences in parameter values

related to sex[38] and age.[39-41] In addition, the use of manually drawn regions of interest in the small pediatric spinal cord may have introduced partial volume contamination, especially in the lower cervical regions.

In this study, youths up to 21 years of age were included to obtain normative values for ages that parallel age groups typically seen in pediatric SCI centers. Although they are not children, youth between 18 and 21 years of age are often in transition from pediatric to adult health care and, in the presence of spinal cord injury, are often cared for in specialized pediatric centers.[42]

Conclusions

This study demonstrated the feasibility of pediatric spinal cord imaging using DTI and produced accurate and reliable DTI measures. Both goals were successfully assessed using an iFOV sequence, which made high-resolution imaging possible, and by including motion correction in the data analysis steps. In future work, the DTI data from the control subjects need to be compared with those of children with SCI and correlated to clinical measures.

Acknowledgments

The authors thank Ms. Laure Rutter for her assistance with subject recruitment.

Disclosures: Scott Faro—*UNRELATED: Grants/Grants Pending:* Shriners.* MJ Mulcahey—*UNRELATED: Grants/Grants Pending:* Shriners Hospitals for Children, Comments: Grant pending and under review. (* *Money paid to institution*).

References

1. National Spinal Cord Injury Statistical Center. **2009 annual statistical report.** University of Alabama at Birmingham, February 2010
2. Brown RL, Brunn MA, Garcia VF. **Cervical spine injuries in children: a review of 103 patients treated consecutively at a level 1 pediatric trauma center.** *J Pediatr Surg* 2001;36:1107–14
3. Osler TM, Vane DW, Tepas JJ, et al. **Do pediatric trauma centers have better survival rates than adult trauma centers? An examination of the national pediatric trauma registry.** *J Trauma* 2001;50:96–101
4. Cirak B, Ziegfeld S, Knight VM, et al. **Spinal injuries in children.** *J Pediatr Surg* 2004;39:607–12
5. Waring WP, Biering-Sorensen F, Burns S, et al. **2009 review and revisions of the international standards for the neurological classification of spinal cord injury.** *J Spinal Cord Med* 2010;33:346–52
6. Mulcahey MJ, Gaughan J, Betz RR, et al. **The international standards for neurological classification of spinal cord injury: reliability of data when applied to children and youths.** *Spinal Cord* 2007;45:452–59
7. Rossi C, Boss A, Lindig TM, et al. **Diffusion tensor imaging of the spinal cord at 1.5 and 3.0 Tesla.** *Rapid Commun* 2007;179:219–24
8. Akter M, Hirai T, Minoda R, et al. **Diffusion tensor tractography in the head-and-neck region using a clinical 3-T MR scanner.** *Acad Radiol* 2009;16:858–65
9. Ducreux D, Fillard P, Facon D, et al. **Diffusion tensor magnetic resonance imaging and fiber tracking in spinal cord lesions: current and future indications.** *Neuroimaging Clin N Am* 2007;17:137–47
10. Kharbanda HS, Alsop DC, Anderson AW, et al. **Effects of cord motion on diffusion imaging of the spinal cord.** *Magn Reson Med* 2006;56:334–39
11. Figley CR, Stroman PW. **Investigation of human cervical and upper thoracic spinal cord motion: implications for imaging spinal cord structure and function.** *Magn Reson Med* 2007;58:185–89
12. Rosenberg DR, Sweeney JA, Gillen JS, et al. **Magnetic resonance imaging of children without sedation: preparation with simulation.** *J Am Acad Child Adolesc Psychiatry* 1997;36:853–59
13. Malisza KL, Martin T, Shiloff D, et al. **Reactions of young children to the MRI scanner environment.** *Magn Reson Med* 2010;64:377–81
14. Mohamed FB, Hunter LN, Barakat N, et al. **Diffusion tensor imaging of the pediatric spinal cord at 1.5T: preliminary results.** *AJNR Am J Neuroradiol* 2011;32:339–45
15. Clark CA, Werring DJ. **Diffusion tensor imaging in spinal cord: methods and applications—a review.** *NMR Biomed* 2002;15:578–86
16. Wilm BJ, Svensson J, Henning A, et al. **Reduced field-of-view MRI using outer volume suppression for spinal cord diffusion imaging.** *Magn Reson Med* 2007;57:625–30
17. Saritas EU, Cunningham CH, Lee JH, et al. **DWI of the spinal cord with reduced FOV single-shot EPI.** *Magn Reson Med* 2008;60:468–73
18. Finsterbusch J. **High-resolution diffusion tensor imaging with inner field-of-view EPI.** *J Magn Reson Imaging* 2009;29:987–93
19. Rieseberg S, Frahm J, Finsterbusch J. **Two-dimensional spatially-selective RF excitation pulses in echo-planar imaging.** *Mag Reson Med* 2002;47:1186–93
20. Ellingson BM, Ulmer JL, Kurpad SN, et al. **Diffusion tensor MR imaging of the neurologically intact human spinal cord.** *AJNR Am J Neuroradiol* 2008;29:1279–84
21. Wheeler-Kingshott CAM, Hickman SJ, Parker GJM, et al. **Investigating cervical spinal cord structure using axial diffusion tensor imaging.** *Neuroimage* 2002;16:93–102
22. Elshafiey I, Bilgen M, He R, et al. **In vivo diffusion tensor imaging of rat spinal cord at 7 T.** *Magn Reson Imaging* 2002;20:243–47
23. Ford JC, Hackney DB, Alsop DC, et al. **MRI characterization of diffusion coefficients in a rat spinal cord injury model.** *Magn Reson Med* 1994;31:488–94
24. Franconi F, Lemaire L, Marescaux L, et al. **In vivo quantitative microimaging of rat spinal cord at 7T.** *Magn Reson Med* 2000;44:893–98
25. Gulani V, Iwamoto GA, Jiang H, et al. **A multiple echo pulse sequence for diffusion tensor imaging and its application in excised rat spinal cords.** *Magn Reson Med* 1997;38:868–73
26. Barakat N, Middleton D, Hunter L, et al. **An investigation of motion correction algorithms for pediatric spinal cord DTI in normals and patients with SCI.** In *Proceedings of the 19th Annual Meeting of ISMRM Montreal, Quebec, Canada, 2011*;6069
27. Le Bihan D, Mangin JF, Poupon C, et al. **Diffusion tensor imaging: concepts and applications.** *J Magn Reson Imaging* 2001;13:534–46
28. Clark CA, Werring DJ, Miller DH. **Diffusion imaging of the spinal cord in vivo: estimation of the principal diffusivities and application to multiple sclerosis.** *Magn Reson Med* 2000;43:133–38
29. Tievsky AL, Ptak T, Farkas J. **Investigation of apparent diffusion coefficient and diffusion tensor anisotropy in acute and chronic multiple sclerosis lesions.** *AJNR Am J Neuroradiol* 1999;20:1491–99
30. Westin CF, Peled S, Gudbjartsson H, et al. **Geometrical diffusion measures for MRI from tensor basis analysis.** In *Proceedings of the 5th Annual Meeting of ISMRM Vancouver, British Columbia, Canada* 1997:1742
31. Alexander AL, Hasan K, Kindlmann G, et al. **A geometric analysis of diffusion tensor measurements of the human brain.** *Magn Reson Med* 2000;44:283–91
32. Shrout PE, Fleiss JL. **Intraclass correlations: uses in assessing rater reliability.** *Psychol Bull* 1979;86:420–28
33. Cascio CJ, Gerig G, Piven J. **Diffusion tensor imaging: application to the study of the developing brain.** *J Am Acad Child Adolesc Psychiatry* 2007;46:213–23
34. Feldman HM, Yeatman JD, Lee ES, et al. **Diffusion tensor imaging: a review for pediatric researchers and clinicians.** *J Dev Behav Pediatr* 2010;31:346–56
35. Lebel C, Walker L, Leemans A, et al. **Microstructural maturation of the human brain from childhood to adulthood.** *Neuroimage* 2008;40:1044–55
36. Hill D, Batchelor P, Holden M, et al. **Medical image registration.** *Phys Med Biol* 2001;46:R1–45
37. Song T, Chen WJ, Yang B, et al. **Diffusion tensor imaging in the cervical spinal cord.** *Eur Spine J* 2011;20:422–28
38. Hsu J, Leemans A, Bai C, et al. **Gender differences and age-related white matter changes of the human brain: a diffusion tensor imaging study.** *Neuroimage* 2008;39:566–77
39. Barnea-Goraly N, Menon V, Eckert M, et al. **White matter development during childhood and adolescence: a cross-sectional diffusion tensor imaging study.** *Cereb Cortex* 2005;15:1848–54
40. Bonekamp D, Nagae LM, Degaonkar M, et al. **Diffusion tensor imaging in children and adolescents: reproducibility, hemispheric, and age-related differences.** *Neuroimage* 2007;34:733–42
41. McGraw P, Liang L, Provenzale JM. **Evaluation of normal age-related changes in anisotropy during infancy and childhood as shown by diffusion tensor imaging.** *AJR Am J Roentgenol* 2002;179:1515–22
42. DeVivo MJ, Vogel LC. **Epidemiology of spinal cord injury in children and adolescents.** *J Spinal Cord Med* 2004, 27[suppl 1]:SS1, S4–10